Supporting Information

What can GNSS tell about physical processes in slowly deforming France? Insights from a community benchmark exercise

M. Métois[1]*, S. Mazzotti[2]*, A. Periollat[3], A. Damon[3]*, J. Grosset[3]*, F. Masson[4], M. Mathey[5], J. Piña-Valdes[6], A. Rigo[7], A. Socquet[6], T. Ueda[8], M. Vergnolle[9], & P. Vernant[3]

**Authors contributed equally, marianne.metois@univ-lyon1.fr; stephane.mazzotti@univ-nantes.fr*

This document presents supplementary figures associated with the paper "What can GNSS tell about physical processes in slowly deforming France? Insights from a community benchmark exercise.". The synthetic velocity fields (either raw or cleaned) and the R-codes used to generate synthetic noise models and available on the EasyData repository https://doi.org/10.57932d194c240-858e-4838-90b5-536b2cbb28fd.

Column	Description	Units
longitude	[-7,12]°E	°
latitude	[38,55]°N	°
$\dot{\epsilon_1}$	First eigen value of the strain rate tensor	/yr
$\dot{\epsilon_2}$	Second eigen value of the strain rate tensor	/yr
$\alpha_{\dot{\epsilon_1}}$	Azimuth of the first eigen vector, taken positive clockwise from North	°
I_1	Divergence, or first invariant of $\dot{\epsilon}$, taken positive for dilation and defined as $\dot{\epsilon_{xx}} + \dot{\epsilon_{yy}}$	/yr
I_2	Second invariant of $\dot{\epsilon}$, defined as $I_2 = \sqrt{\dot{\epsilon}_{xx}^2 + \dot{\epsilon}_{yy}^2 + 2\dot{\epsilon}_{xy}^2}$	/yr
ω	Vorticity defined as $\omega = \partial_y v_x - \partial_x v_y$	/yr
$\dot{\epsilon_{xx}}$	first diagonal component of $\dot{\epsilon}$	/yr
$\dot{\epsilon_{yy}}$	second diagonal component of $\dot{\epsilon}$	/yr
$\dot{\epsilon_{xy}}$	non diagonal component of $\dot{\epsilon}$	/yr

Tab. S1: Description of the outputs needed to properly integrate strain rates calculations in our exercise. Note that the three last lines are facultative. When given, it allows to check wether the invariants have been correctly computed.

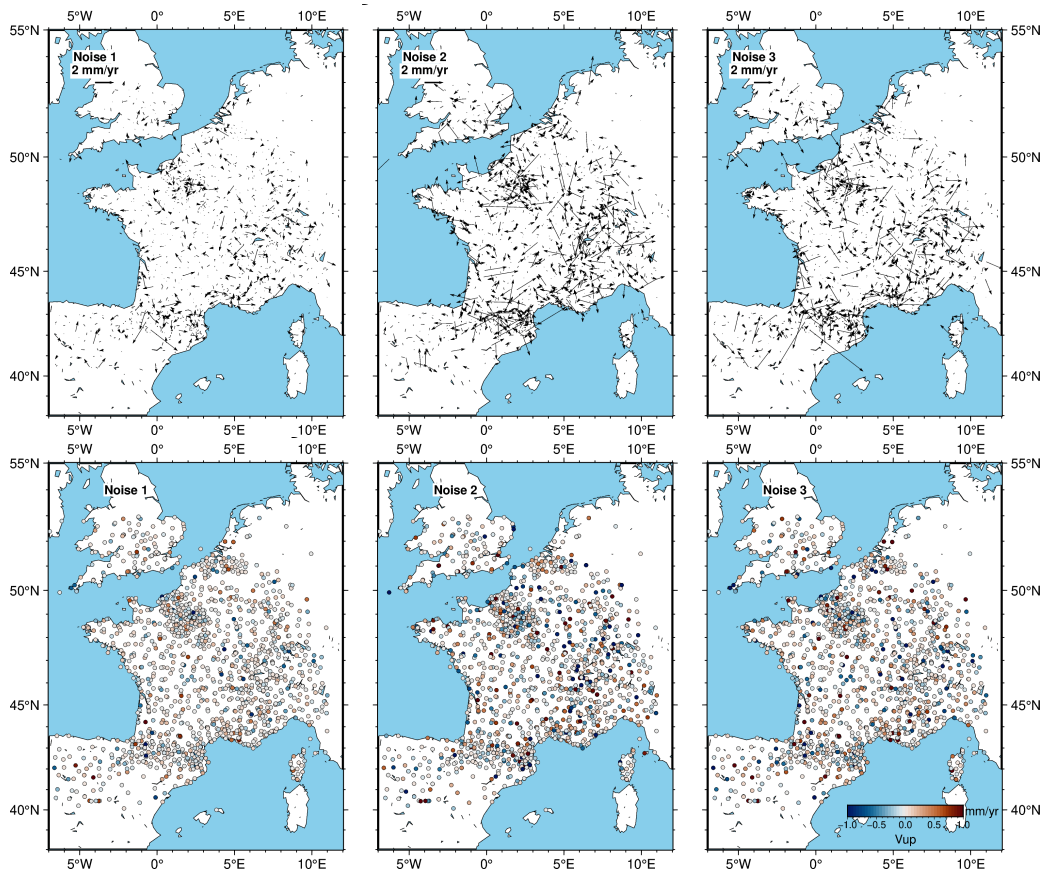

Fig. S1: Synthetic noise models on the horizontal (top) and vertical (bottom) components of the velocity field. Noise models 1, 2 and 3 are presented from left to right.

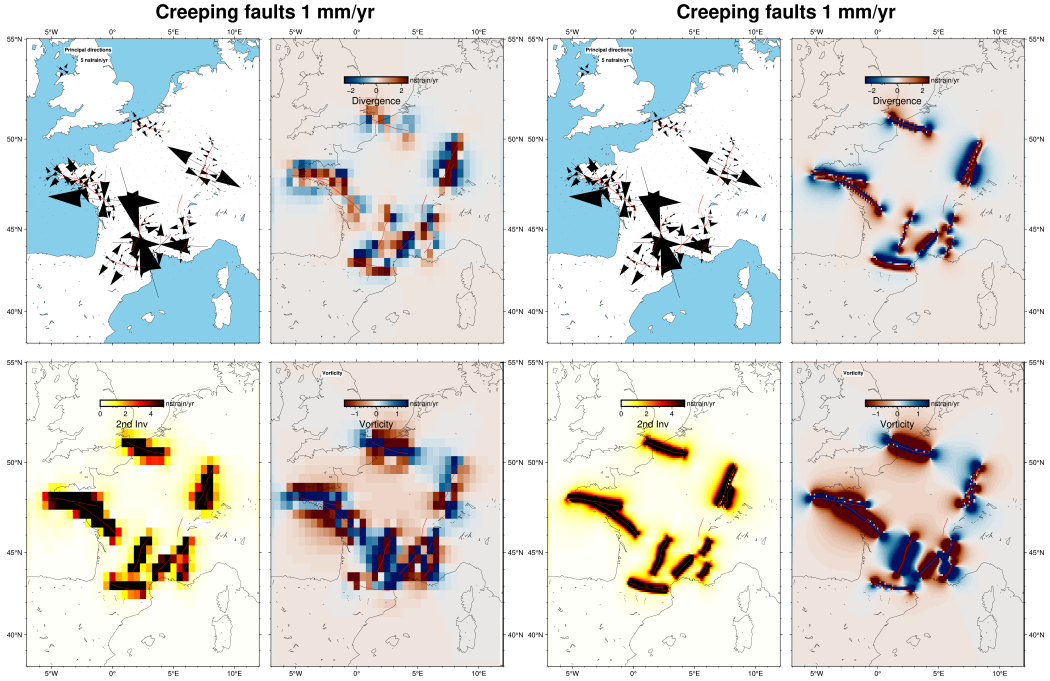

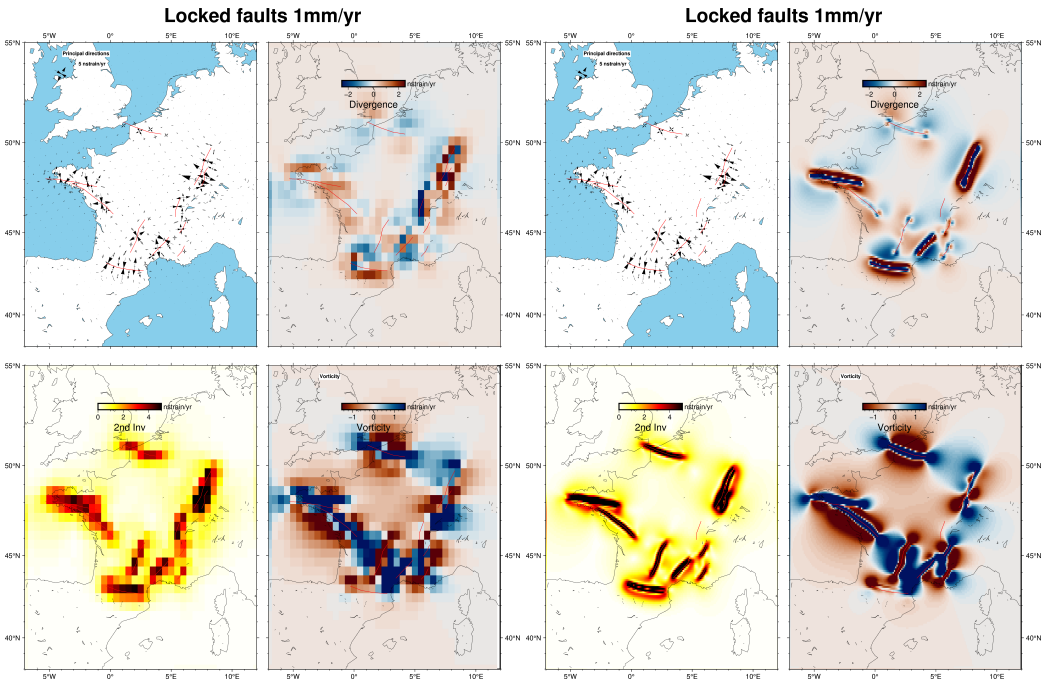

Fig. S2: Theoretical principal components of the strain rates tensor, divergence, I_2 and vorticity for model 5 (up) and 6 (bottom) sampled over 0.5° (left) or 0.1°(right) grids.

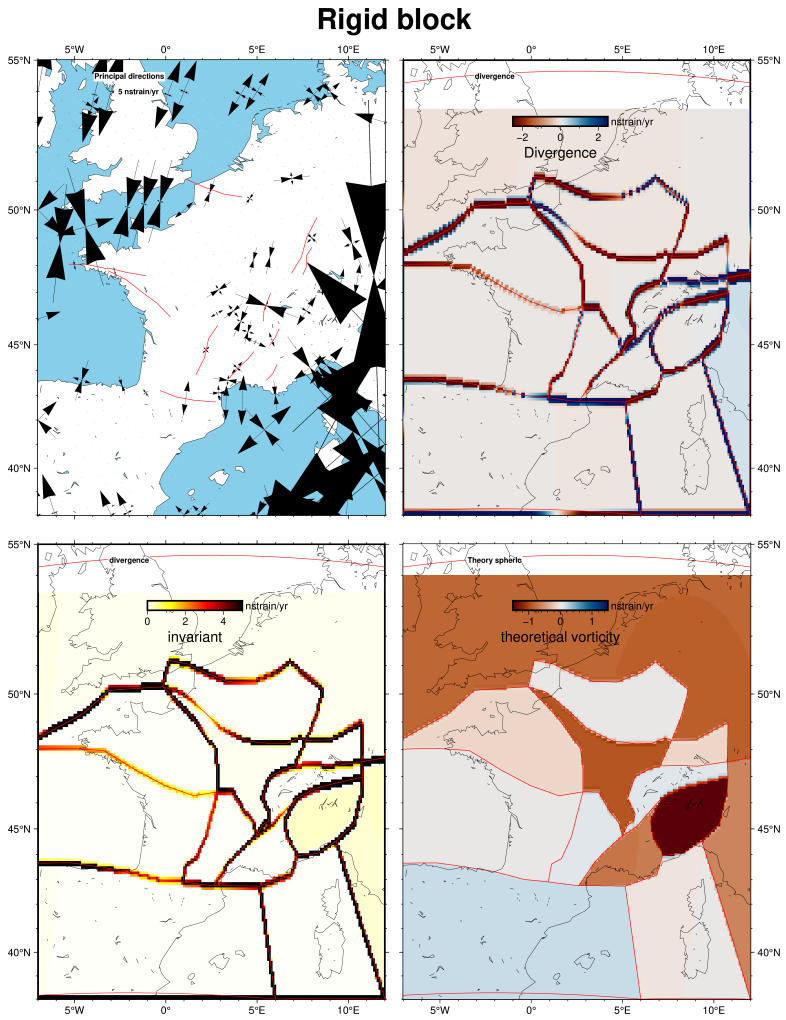

Fig. S3: Theoretical principal components of the strain rates tensor, divergence, I_2 and vorticity for model 7.

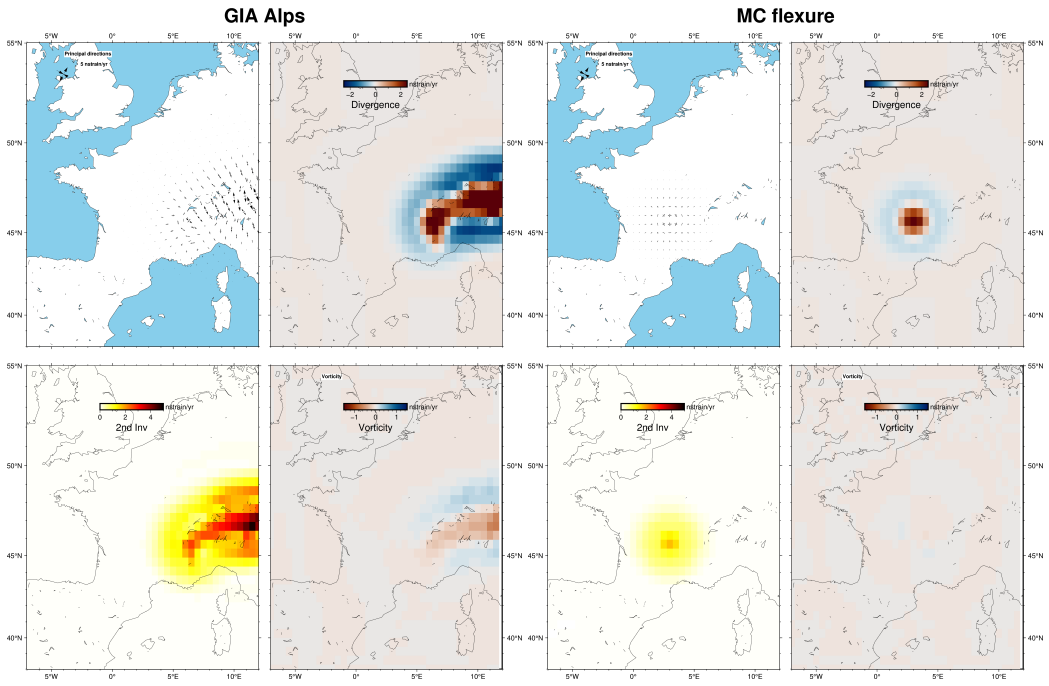

Fig. S4: Same than fig S3 but for model 8 (left) and 9 (right).

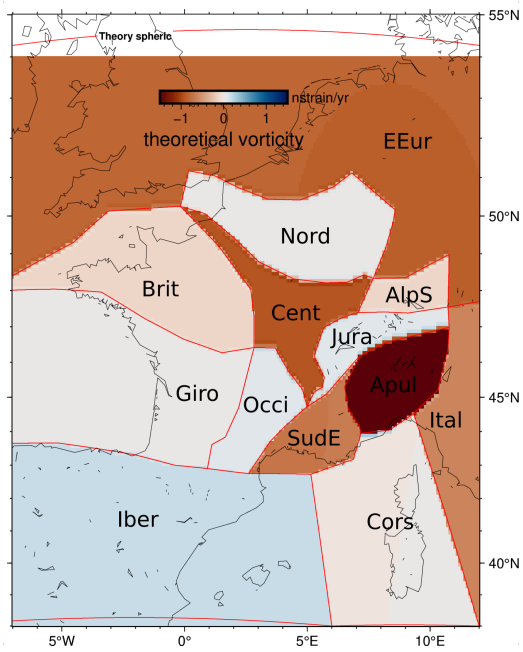

Fig. S6: Names of the rigid blocks used in model 7, associated with Eulerian poles listed in table S2.

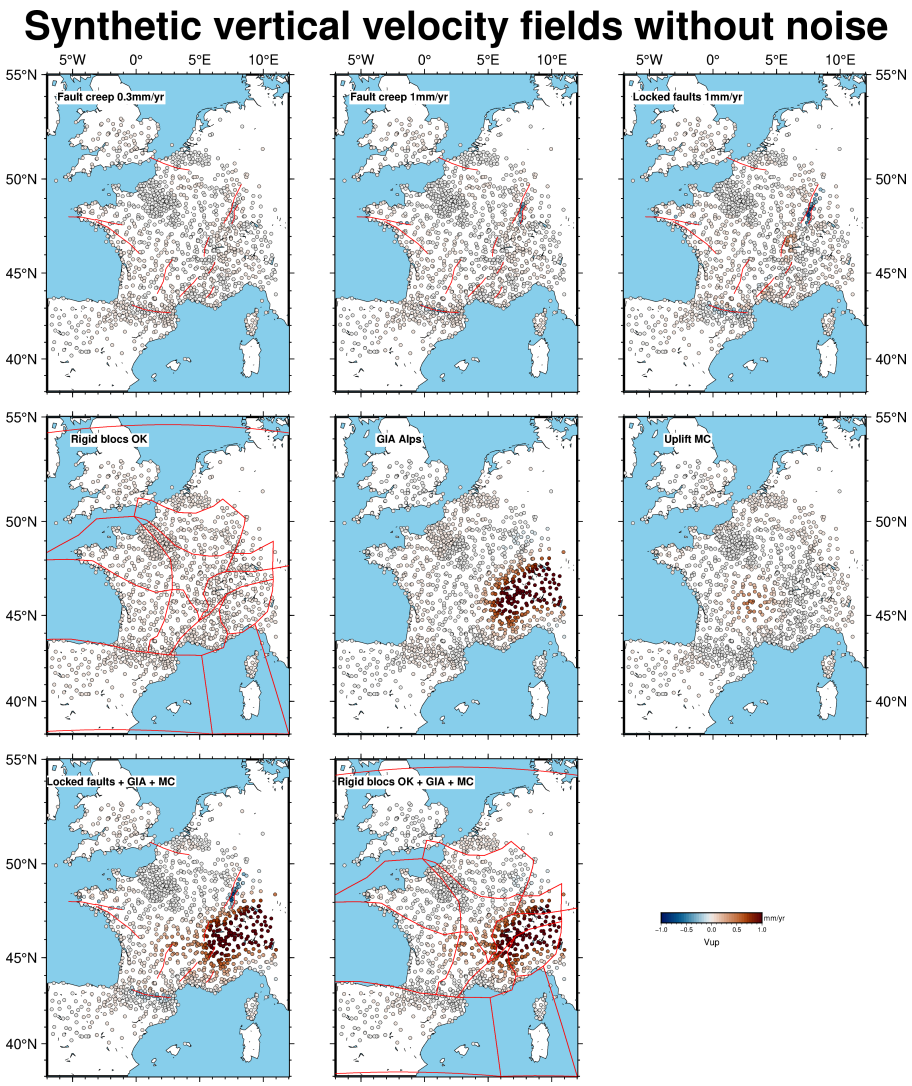

Fig. S5: Synthetic vertical velocity field for models 4 to 11 without noise.

Block	lon (°E)	lat (°N)	ω °/Myr
Nord	203.142	8.102	0.00199
Jura	181.412	-41.657	0.0314
Cent	324.998	73.795	0.00359
Brit	8.385	48.940	0.0278
Giro	160.767	-45.595	0.0031
Occi	4.428	49.356	0.03036
SudE	189.744	-37.546	0.0126
Apul	0.984	44.422	0.02365
Iber	198.305	-47.508	0.01337
Cors	272.715	8.312	0.00274
EEur	326.139	43.476	0.00482
AlpS	7.304	45.652	0.17424
Ital	326.649	37.230	0.02818

Tab. S2: Eulerian poles associated with theoretical rigid blocks displayed in figure S6 and used in model 7.

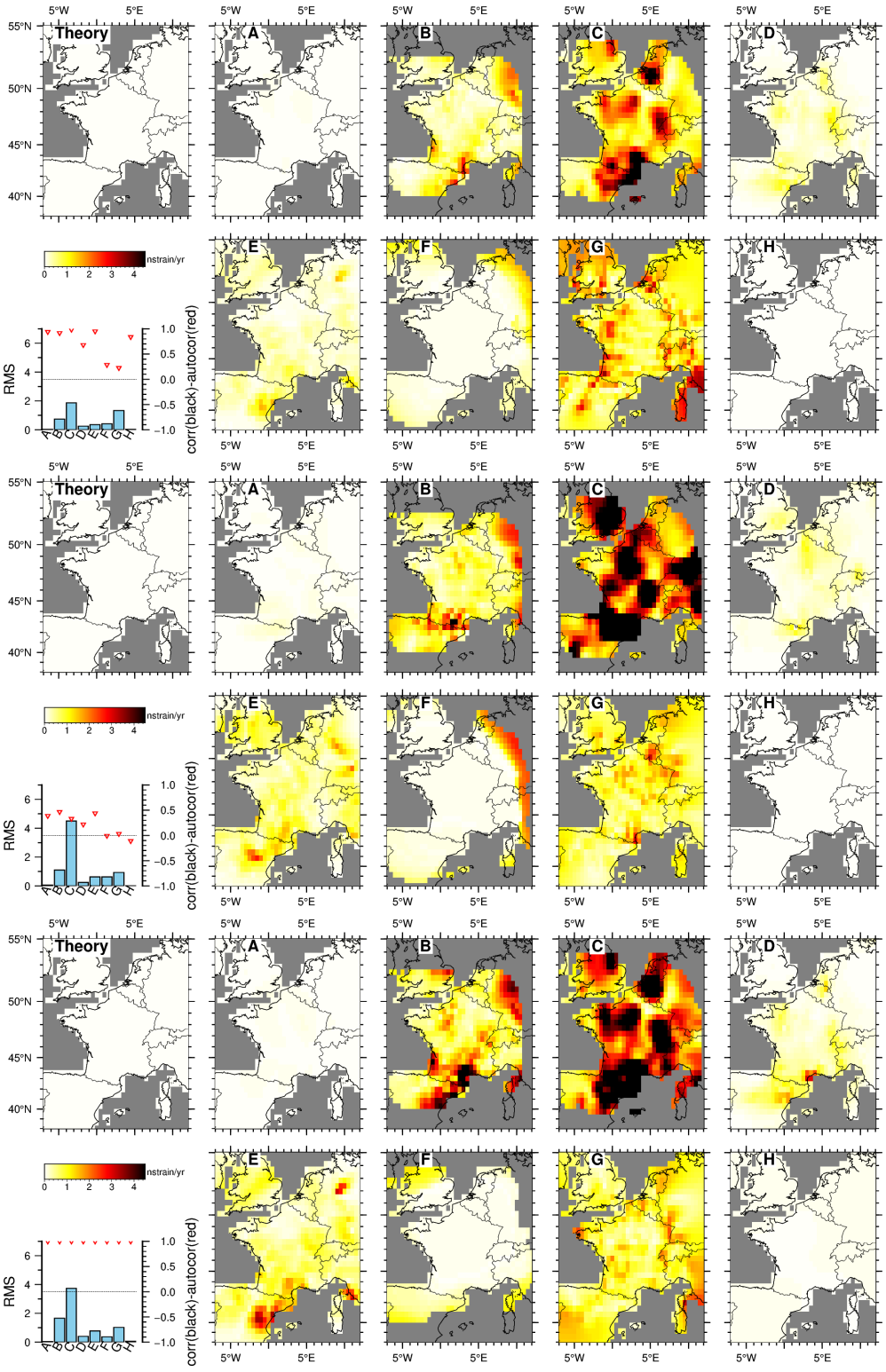

Fig. S7: Maps of theoretical (upper left panel) and retrieved (onshore only) I_2 for noise models 1 (top), 2 (middle), and 3 (bottom). Upper left graphs show computed standard statistics. Correlation cannot be computed with entirely null theoretical map, while autocorrelation is computed with respect to retrieved values for model 3 (reference noise model).

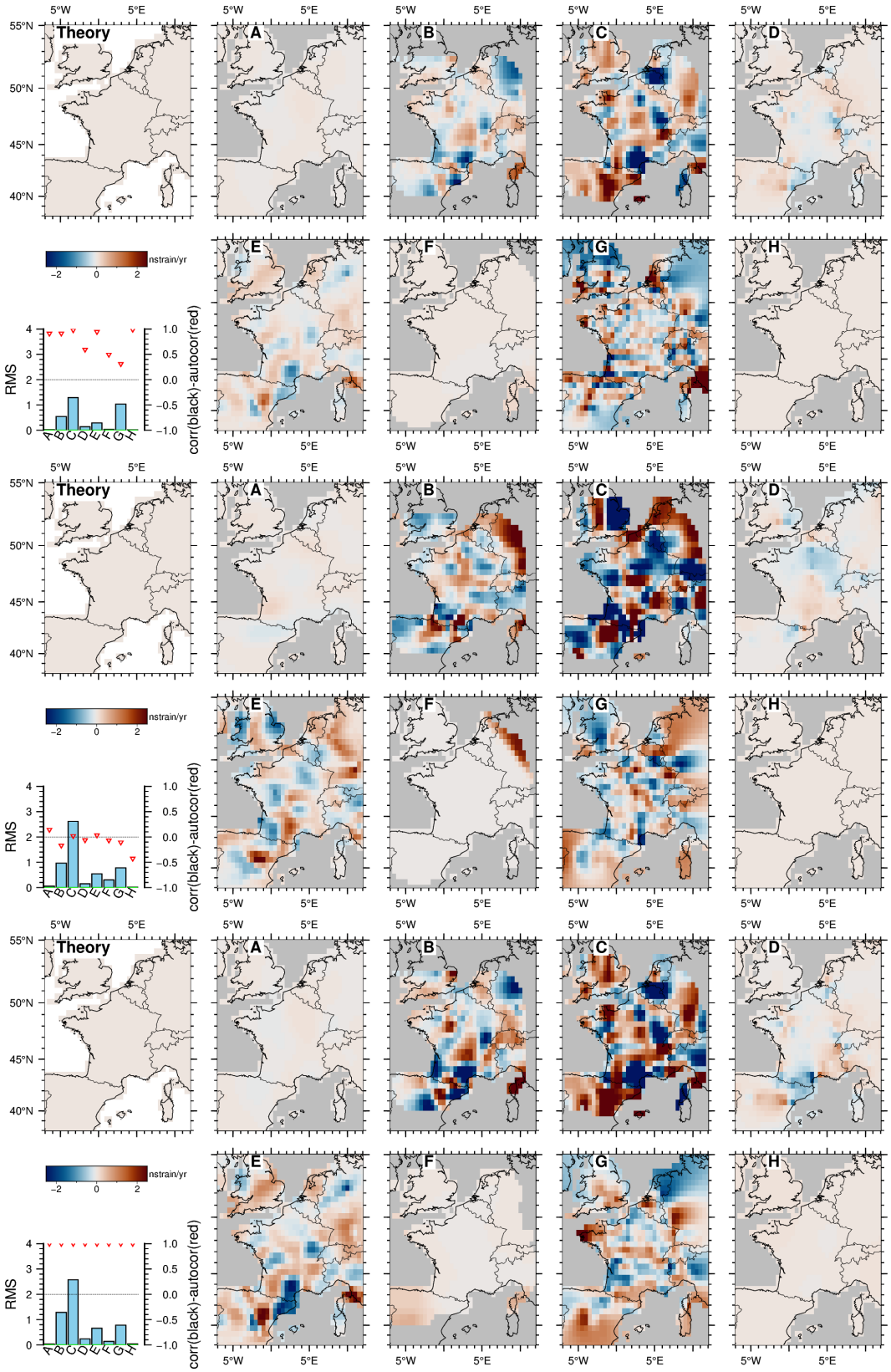

Fig. S8: Same than figure S7, but for divergence.

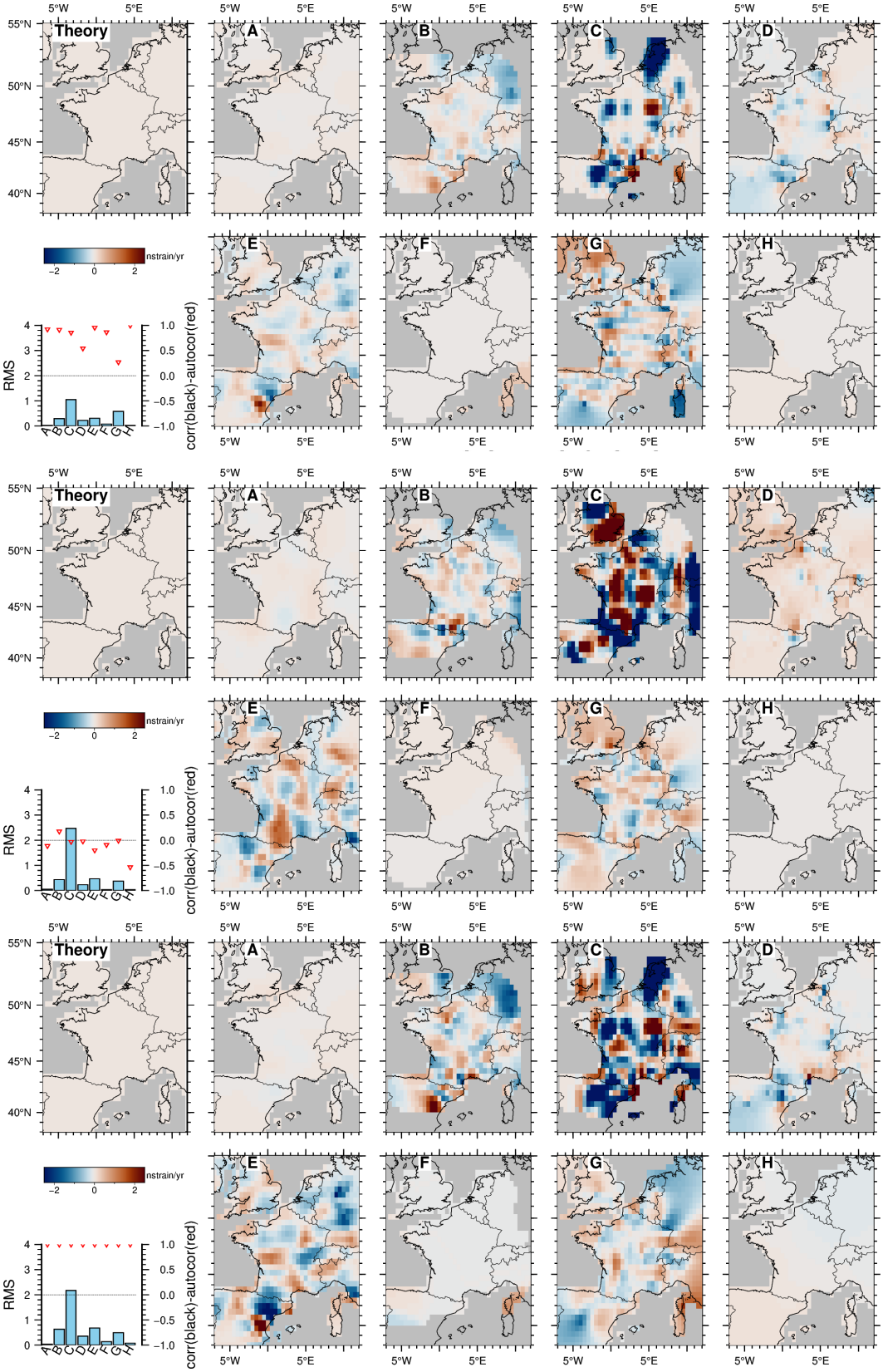

Fig. S9: Same than figure S7, but for vorticity.

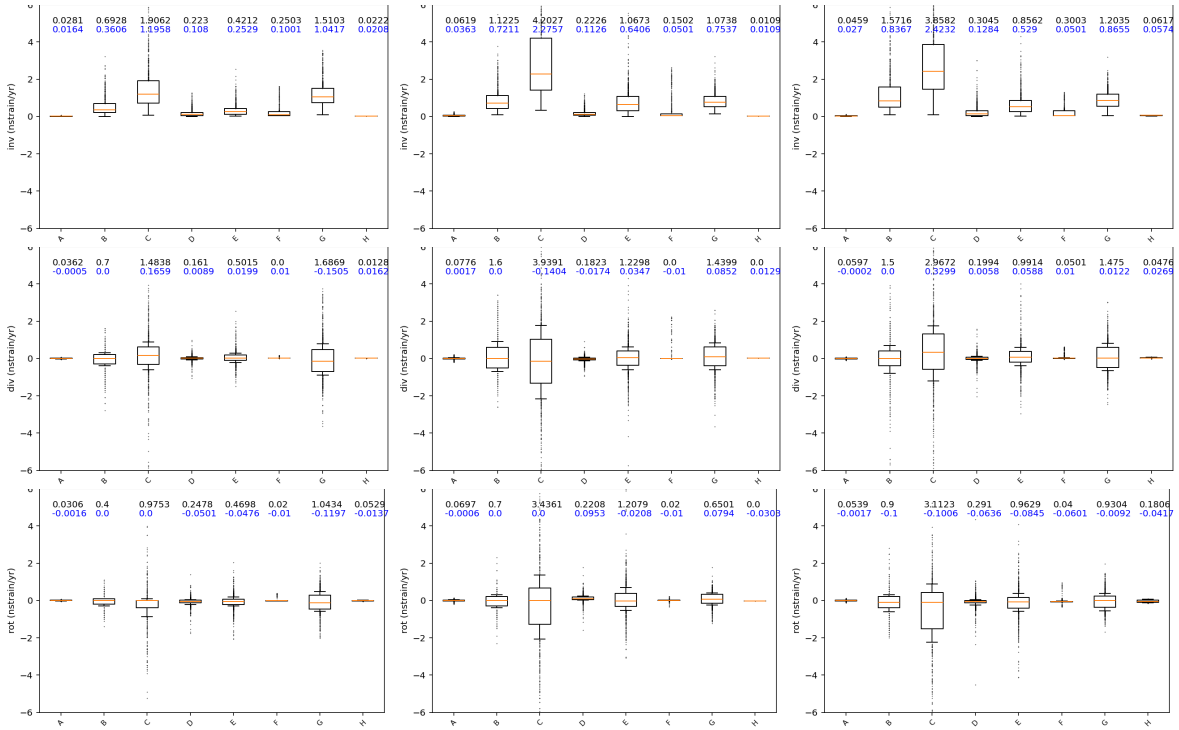

Fig. S10: Boxplot graphs representing the dispersion of the results obtained by each contribution (A to H) for noise model 1 (left), 2 (center) and 3 (right) for I_2 (top), divergence (middle) and vorticity (bottom). Orange bar is the median of the distribution, black and blue values on top stand for IQR 90% and median value, respectively.

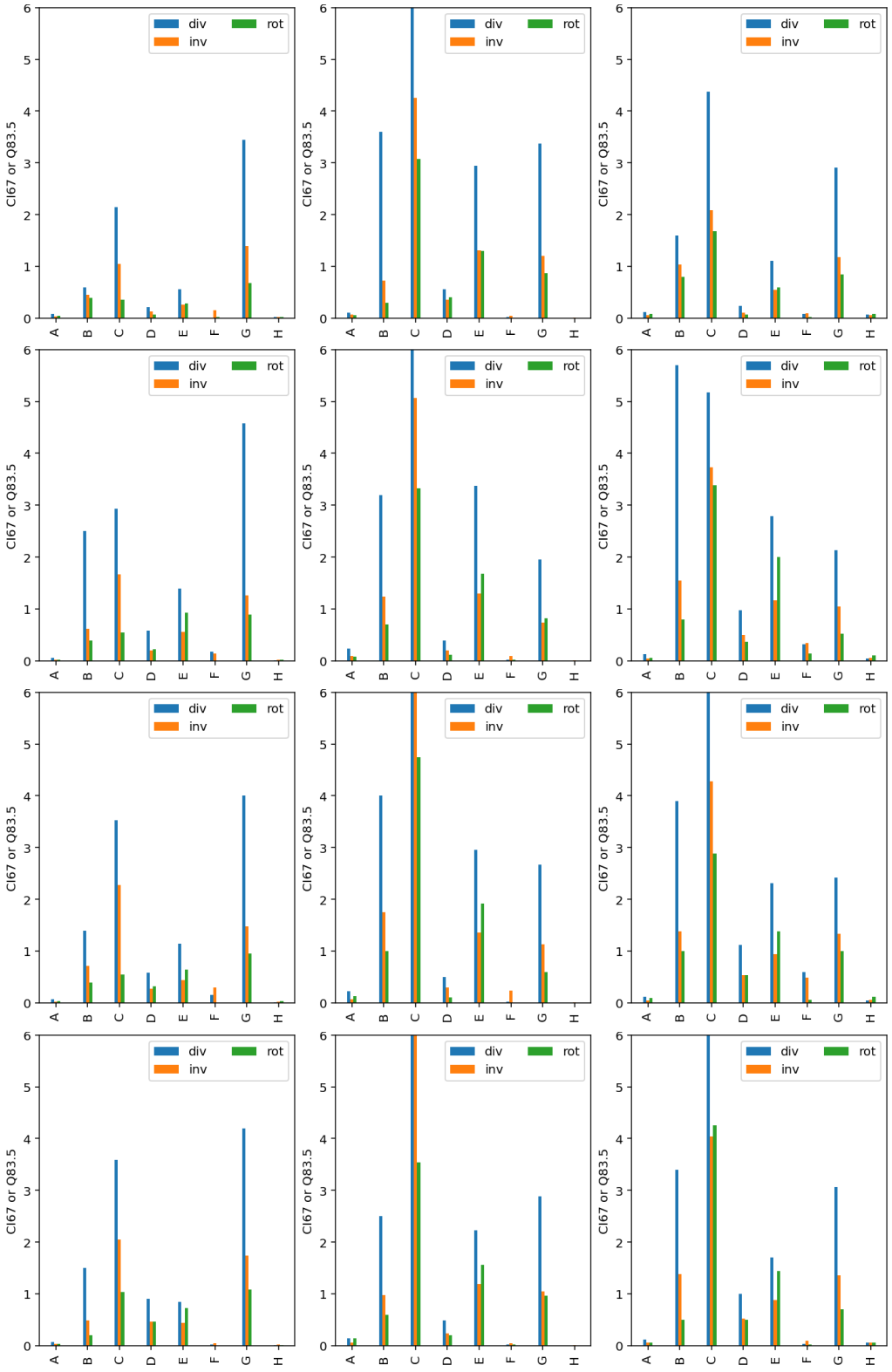

Fig. S11: Same as figure 4 but for geographical boxes plotted in figure 1, from top to bottom : Alps, Pyrenees, Armorican massif, Paris Basin.

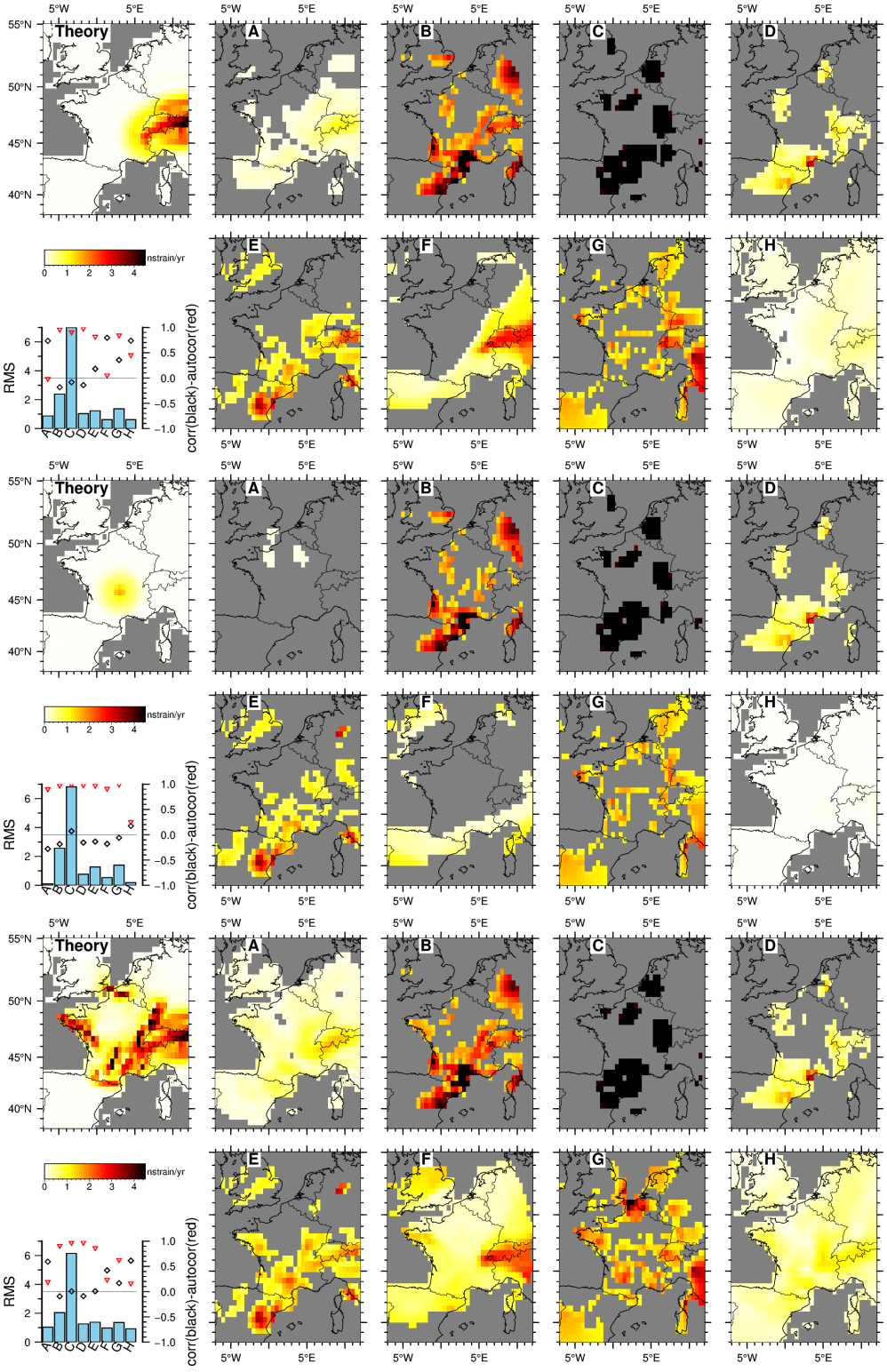

Fig. S12: Maps of theoretical (upper left panel) and retrieved (onshore only) I_2 for noise models 8 (Alpine GIA, top), 9 (Central massif hot spot, middle), and 10 (combined, bottom). Retrieved maps are masked based on the threshold values determined in section 4.1 and table 3. Lower left graphs show computed standard statistics. Autocorrelation is computed with respect to retrieved values for model 3 (reference noise model).

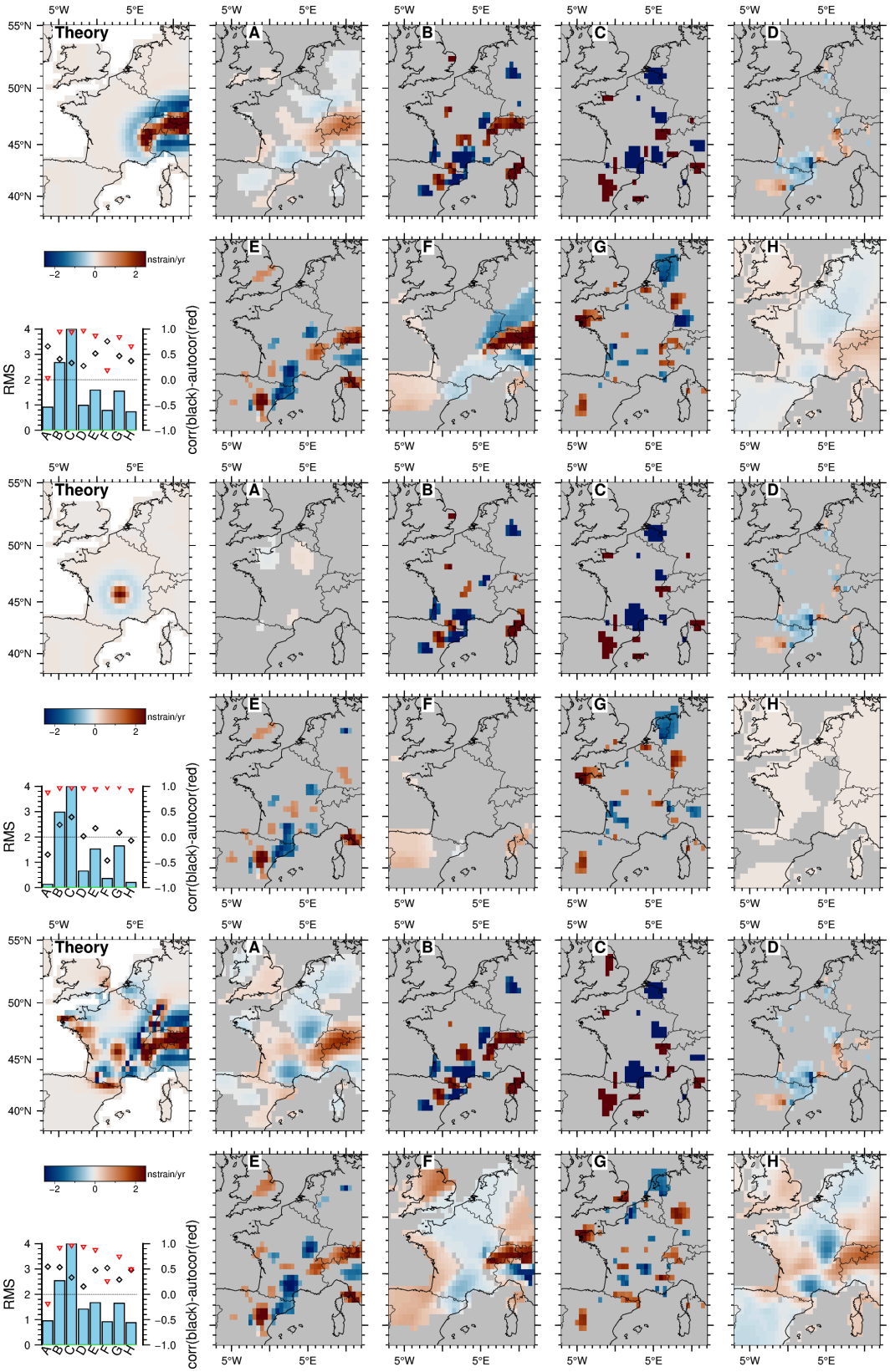

Fig. S13: Same than figure S12 but for divergence.

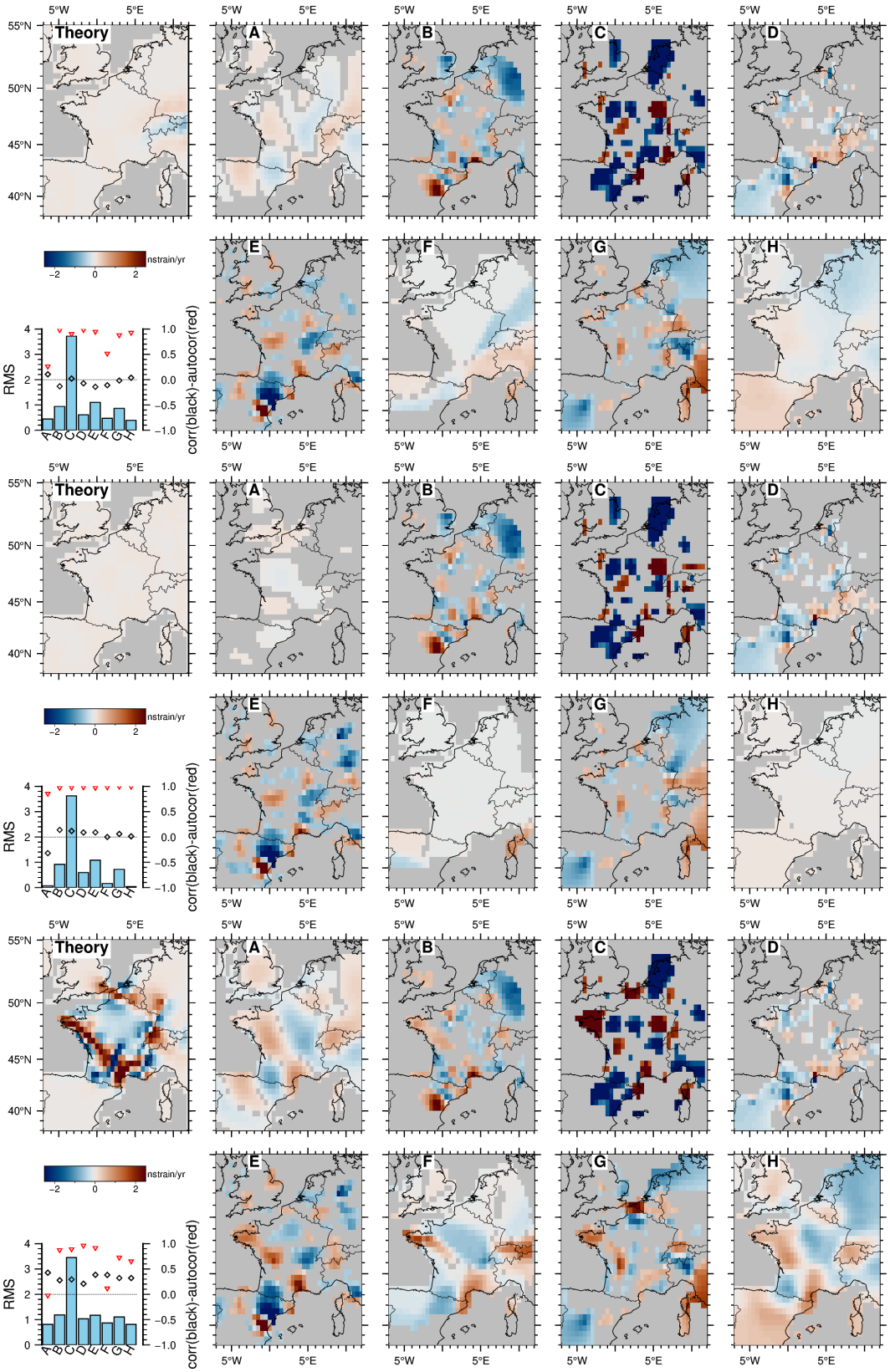

Fig. S14: Same than figure S12 but for vorticity.

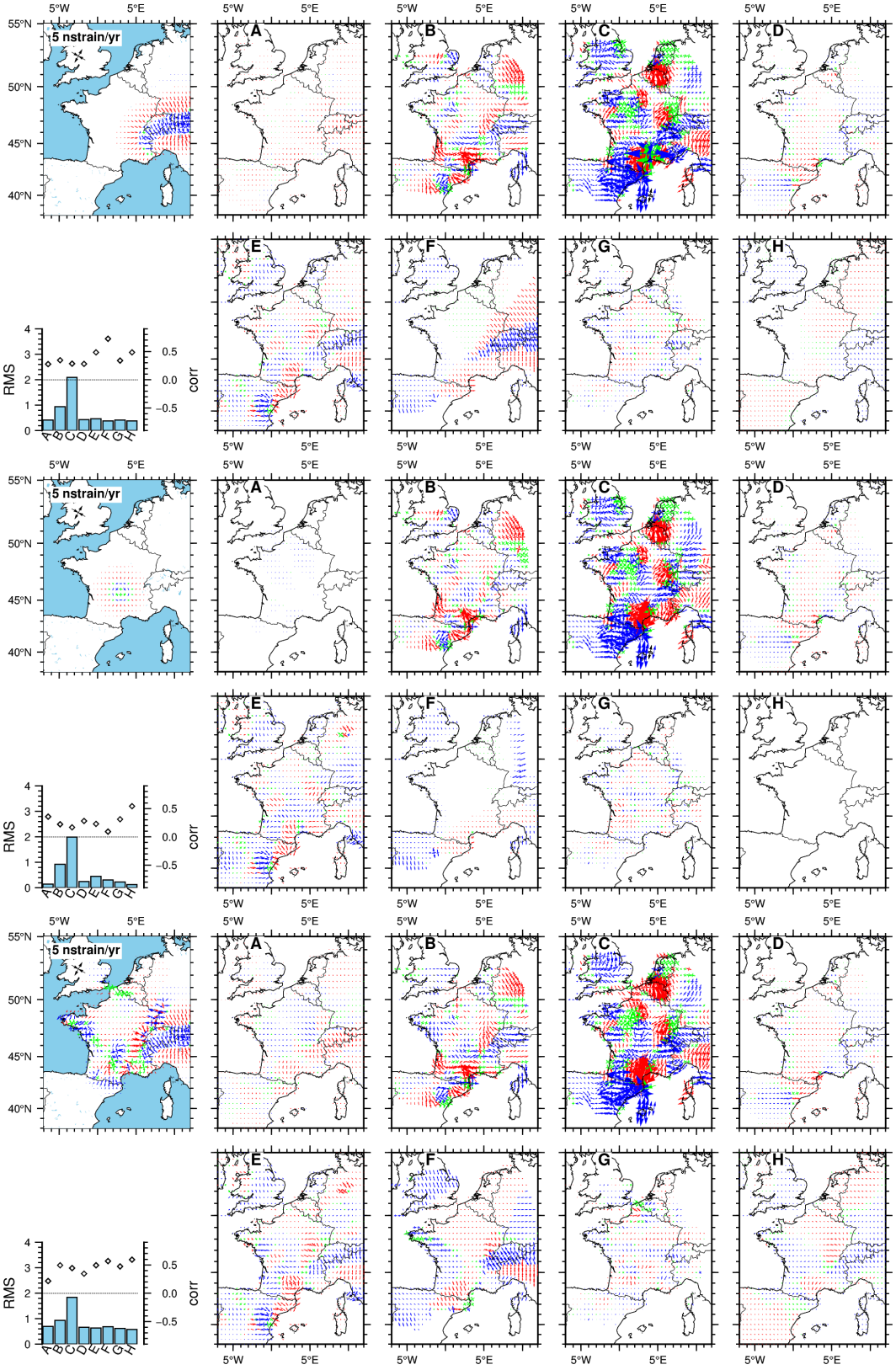

Fig. S15: Same as figure S12 but for principal directions. For clarity, tectonic style based on the ϵ_1/ϵ_2 ratio is color-coded (blue - extension, red - compression, green - strike slip).

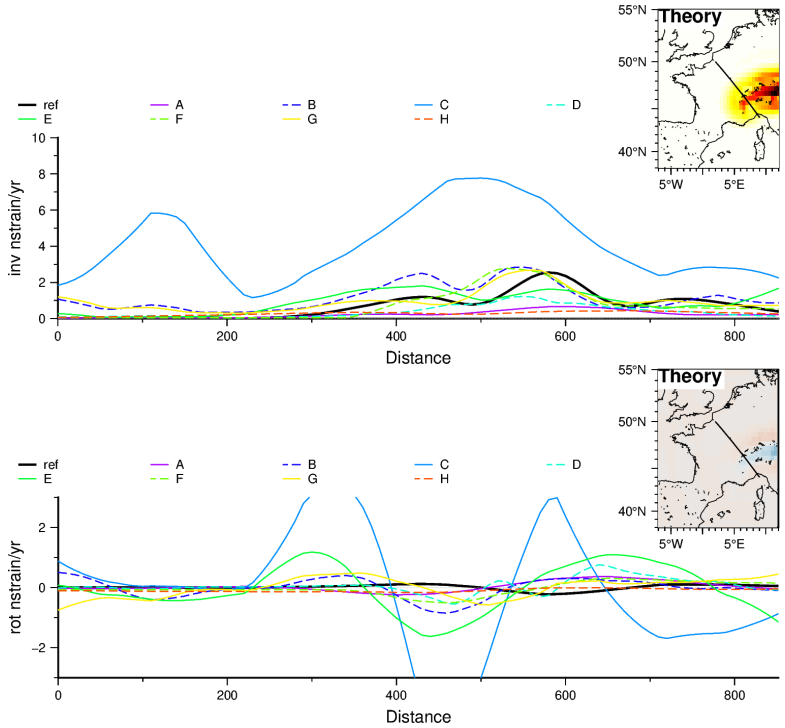

Fig. S16: Profile view of expected (black bold line) versus retrieved I_2 (top) and vorticity (bottom), along a profile line crossing the Alpine chain for model 8. Values originally sampled on a 0.5° grid have been interpolated.

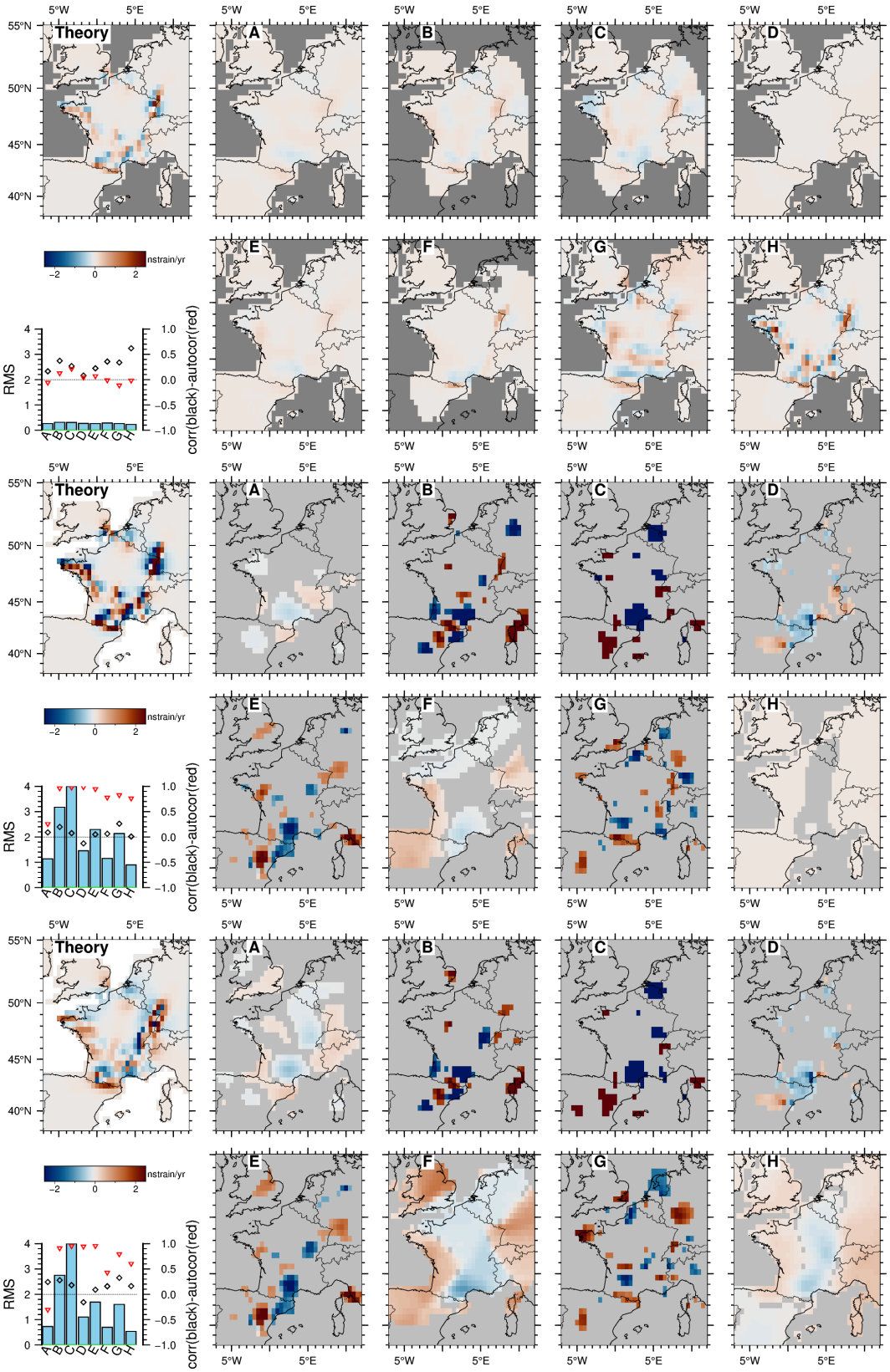

Fig. S17: Same as figure 7 but for divergence.

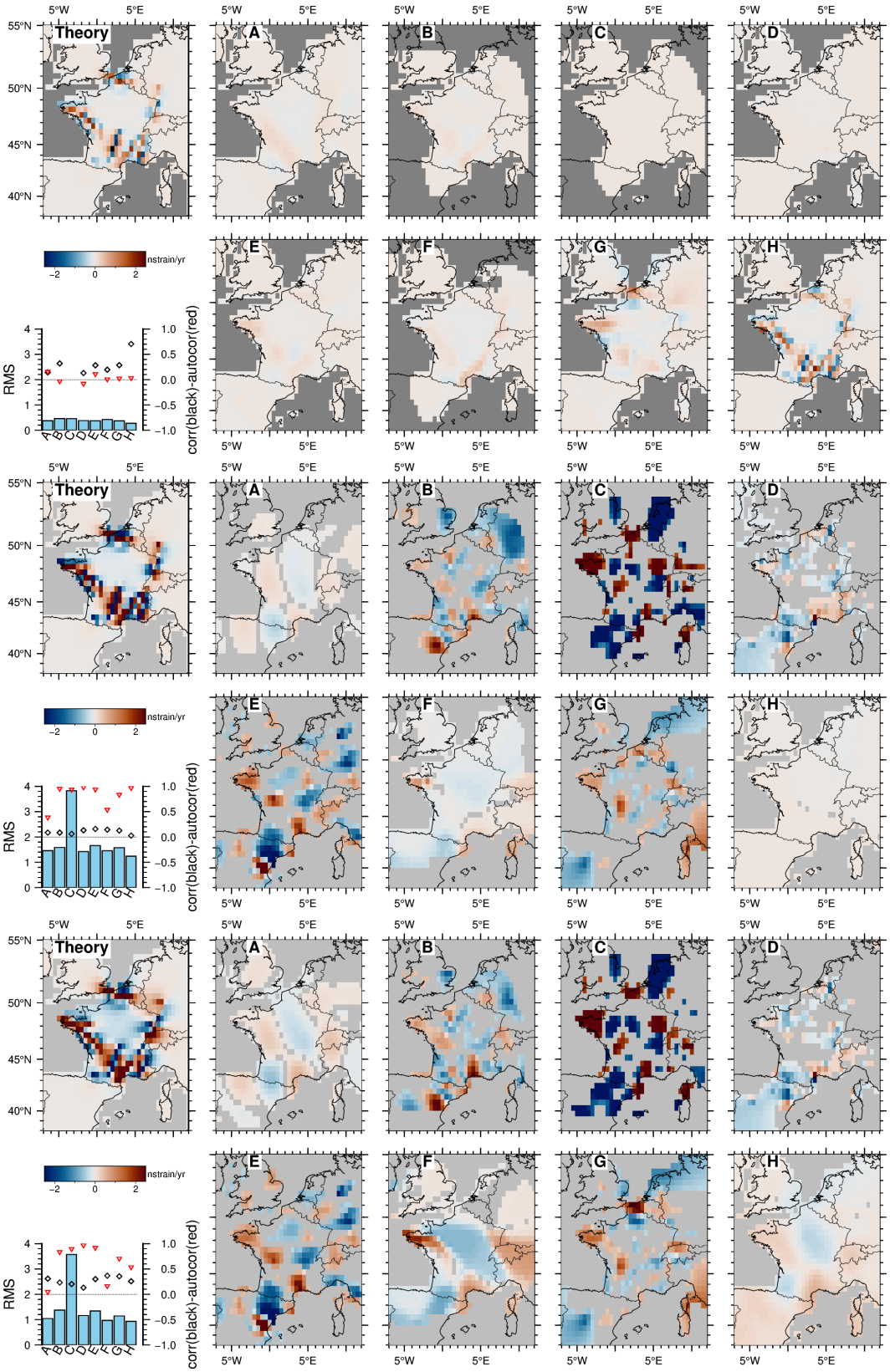

Fig. S18: Same as figure 7 but for vorticity.

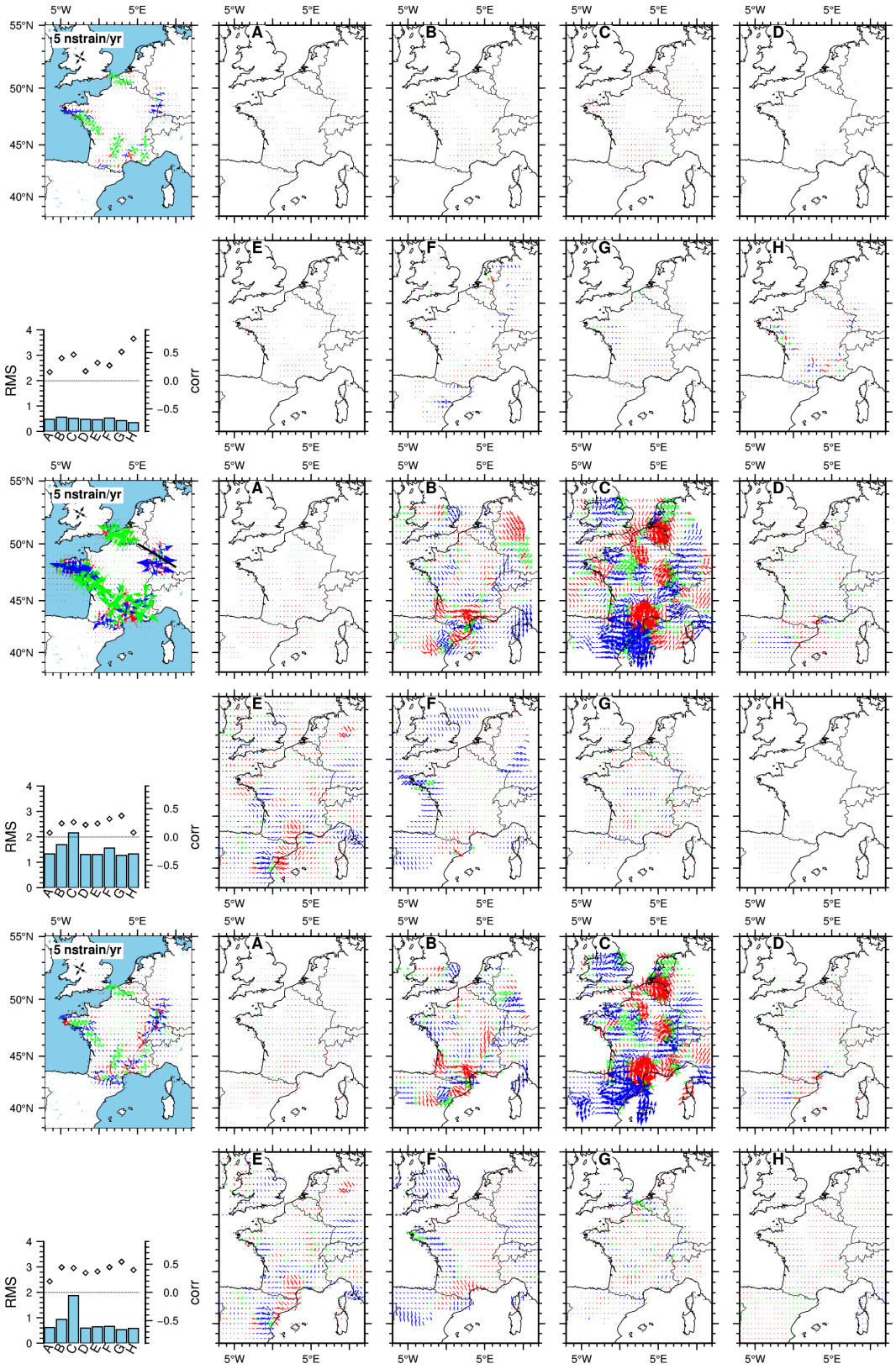

Fig. S19: Same as figure 7 but for principal directions. For clarity, tectonic style based on the ϵ_1/ϵ_2 ratio is color-coded (blue - extension, red - compression, green - strike slip).

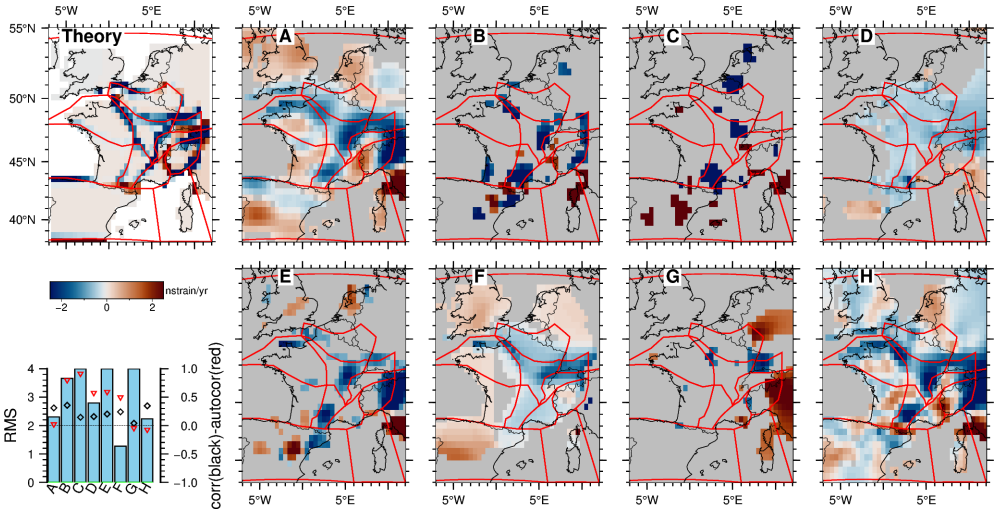

Fig. S20: Same as figure 8 but showing theoretical and retrieved divergence for model 11.

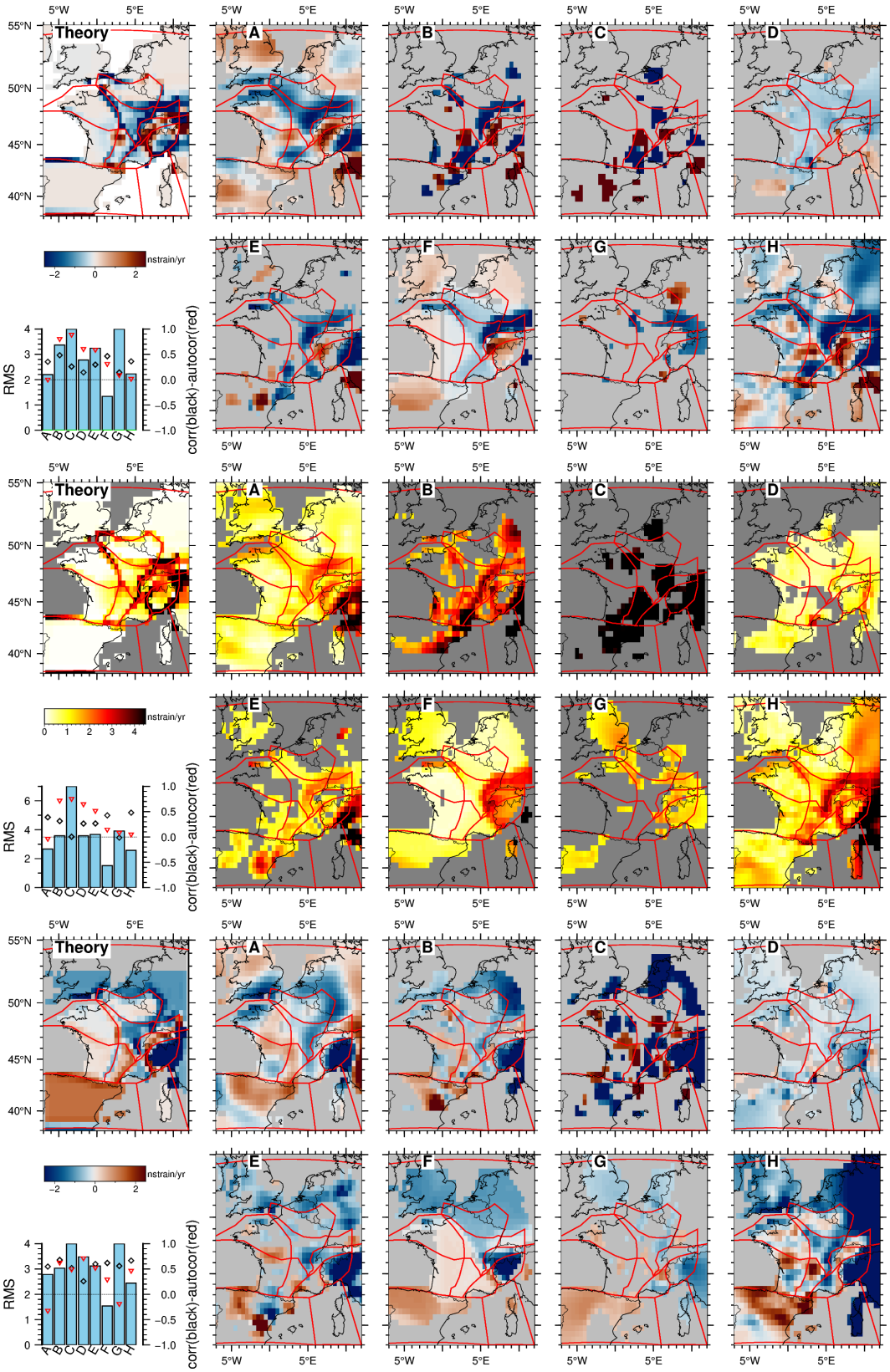

Fig. S21: Same as figure 8 but for model 7.

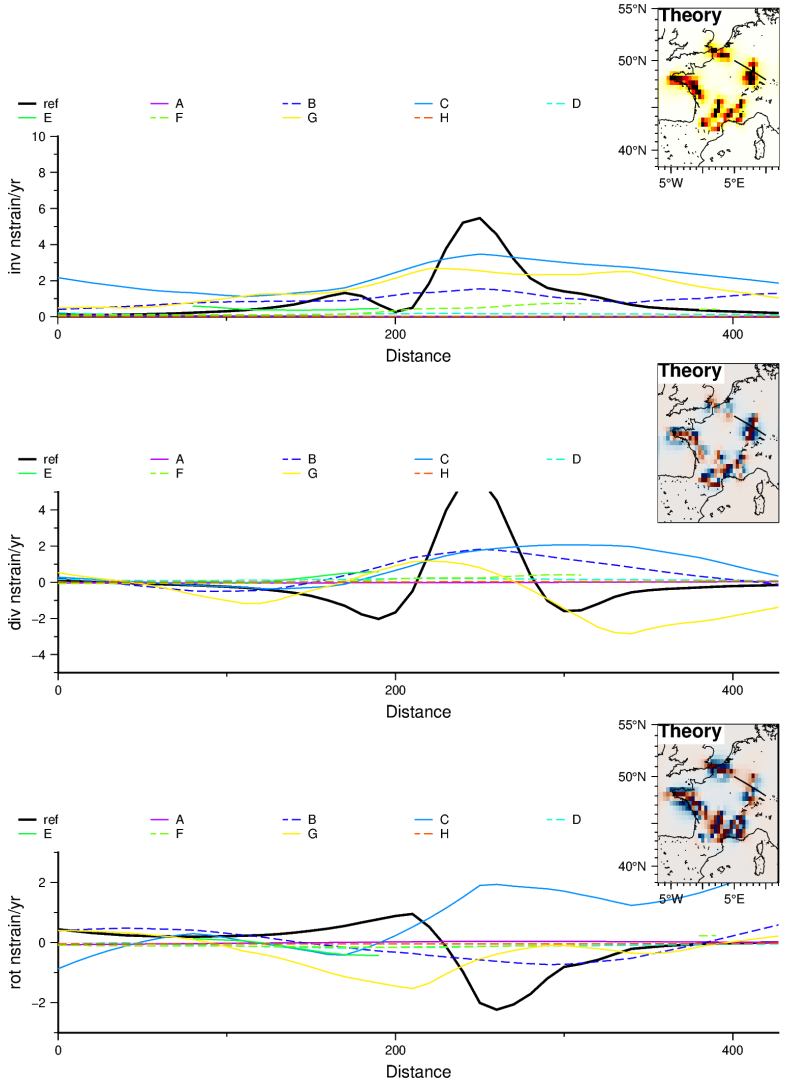

Fig. S22: Profile view of expected (black bold line) versus retrieved strain rate indicators I_2 (top), divergence (middle) and vorticity (bottom), along a profile line crossing the Rhine graben for model 5. Values originally sampled on a 0.5° grid have been interpolated.

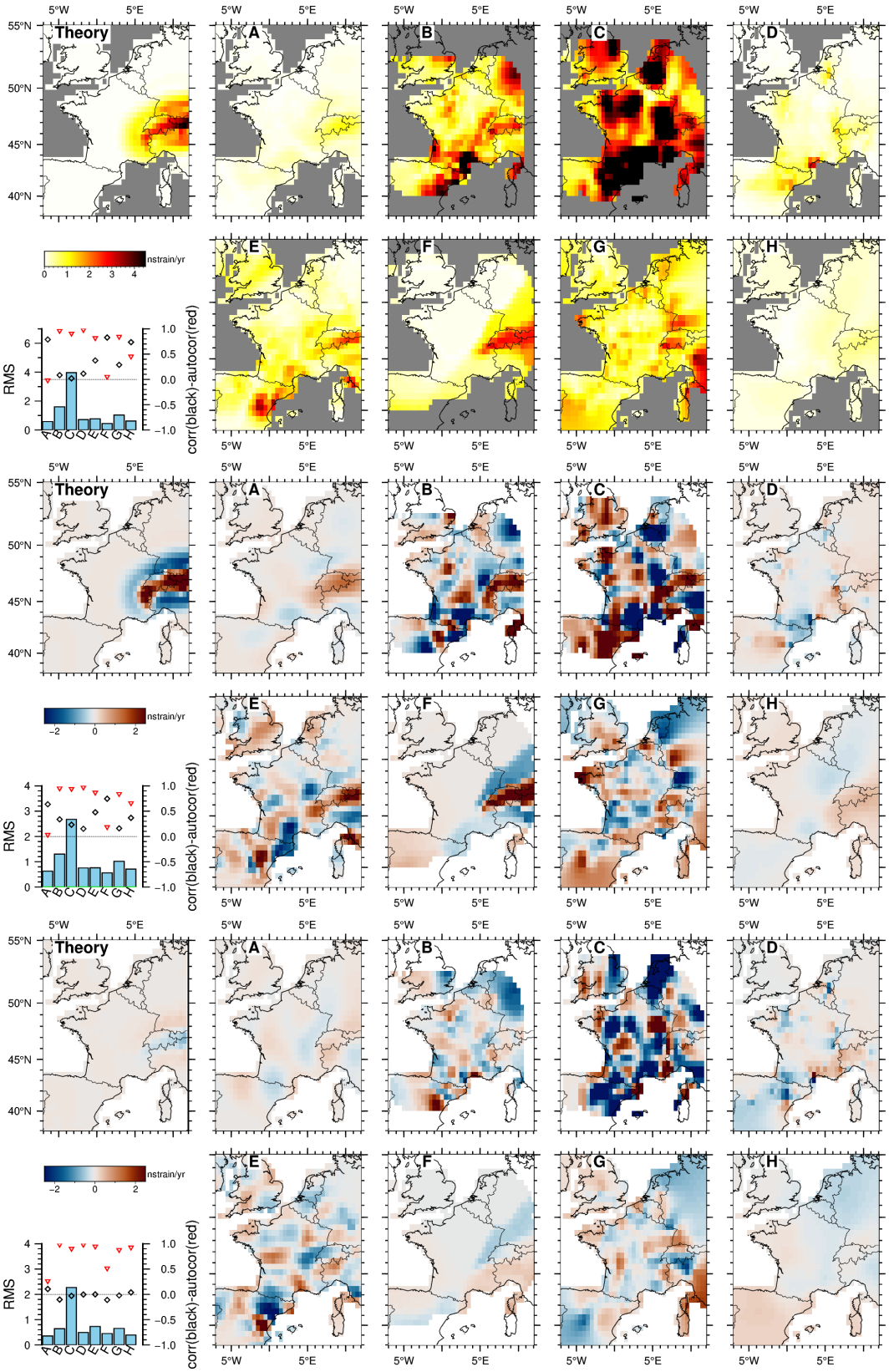

Fig. S23: Entire maps of theoretical (upper left panel) and retrieved (onshore only) I_2 (top), divergence (middle) and vorticity (bottom) for model 8 (Alpine GIA). Lower left graphs show computed standard statistics. Autocorrelation is computed with respect to retrieved values for model 3 (reference noise model).

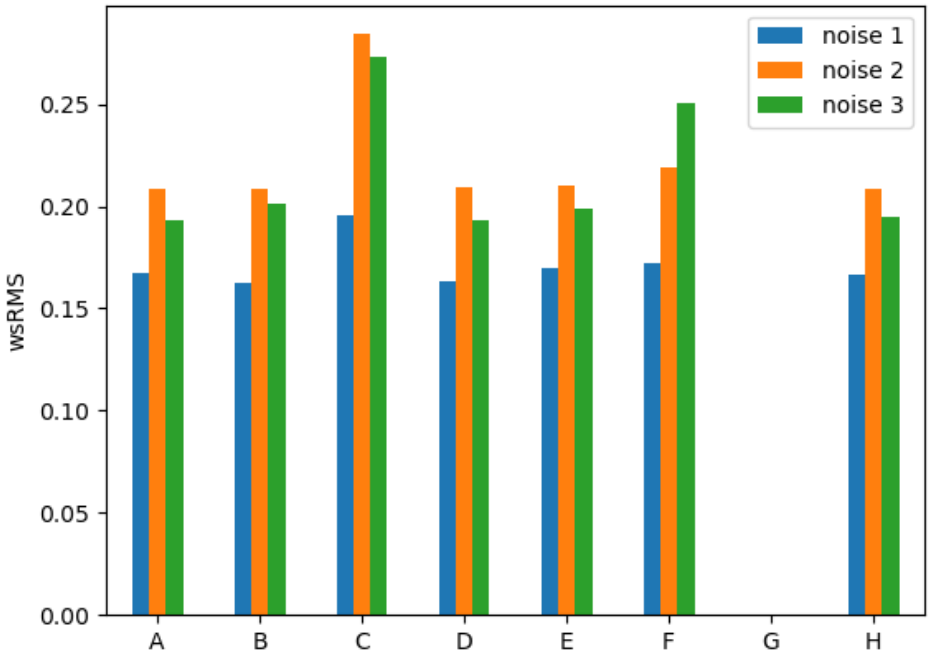

Fig. S24: wRMS computed between observed (v_{obs}) and predicted (v_{pred}) velocities for each method allowing for this comparison, and each noise model. wRMS is given by $\sqrt{\frac{1}{\sum_1^{2N}\frac{1}{\sigma^2}}\sum_1^{2N}\frac{(v_{obs}-v_{pred})^2}{\sigma^2}}$, where N is the number of stations.